Available online at www.sciencedirect.com
ScienceDirect
Mendeleev Commun., 2011, **21**, 312–314
Mendeleev Communications

Direct preparation of anion-free pure silver hydrosols

Anna A. Semenova,[a] Eugene A. Goodilin*[a,b] and Yuri D. Tretyakov[a,b]

[a] *Department of Materials Science, M. V. Lomonosov Moscow State University, 119991 Moscow, Russian Federation*
[b] *Department of Chemistry, M. V. Lomonosov Moscow State University, 119991 Moscow, Russian Federation. Fax: +7 495 939 0998; e-mail: Goodilin@gmail.com*

DOI: 10.1016/j.mencom.2011.11.006

The simplest preparation method of stable sols of naked 2–90 nm pure silver nanoparticles in water is suggested for the first time using silver(I) oxide without reducing agents or anionic pollutants.

The known methods of silver sol preparation are numerous[1–7] because this nanomaterial becomes popular in medicine[8,9] and medical diagnostics[10] like the SERS (surface enhanced Raman spectroscopy) detection of single biomolecules or other analytes.[11,12] At the same time, it is usually difficult to remove trace impurities like borates, if for instance $NaBH_4$ is traditionally used,[1] or products of oxidizing organic compounds,[4,5] or cytotoxic anions like NO_3^- in the case of a silver nitrate soluble precursor. It is evidently possible to apply an additional purification step, such as ultracentrifuges and ultrasonic re-dispersing of precipitated nanoparticles, or to remove anions and pollutants by dialysis. However, it is also possible to get then enlarged aggregates of silver nanoparticles or coagulated sols. Thus, it remains important to search for new robust, cheap and user-friendly methods for preparation of silver nanoparticles. In this paper, to the best of our knowledge, the simplest preparation of naked 2–90 nm pure silver nanoparticles in pure water is suggested for the first time using silver(I) oxide soluble complexes without reducing agents or anionic pollutants; the method is referred to as a PUSH (pure silver hydrosol) one.

Silver oxide is a well-known compound,[13] which is unique in terms of the purpose of this work because it consists of components of the system under question only, namely, silver and oxygen, constituting also a water solvent; the decomposition temperature of Ag_2O is about 150–300 °C in a dry state; finally, Ag_2O is only partly soluble in water and precipitates from Ag^+ solutions when treated by alkali metal hydroxides, and then it can be easily purified by washing with small portions of distilled water. The remaining point is that silver(I) oxide can be transferred into a clean transparent solution if aqueous NH_3 is used to form water-soluble complexes. All the described advantages were experimentally applied in this work with an additional stage of silver(I) oxide complexes decomposition in boiling water under the conditions of fixed silver content and controlled decomposition time.[†]

All the resulting sols were yellow-brownish with different intensities of their colors as dependent mostly on the initial silver(I) oxide complex concentration in hot water. First signs of coloring could be observed already after 10–15 min upon the injection of the complex into boiling water, and the color becomes more intense in time. Finally, after an hour, a reflecting metallic silver film could be observed on water surface for the most concentrated solution although the solution remained dark-brownish in the bulk. All the sols were odorless and stable for at least several days. Their drying at room temperature gives no crystals of remaining silver(I) oxide while nanoparticle sol forms a thin and smooth silver layer. Probably some amount of aqueous NH_3 still remains in the sols despite of water boiling and abrupt falling of NH_3 solubility since pH exceeds 7 in several cases (Table 1). Indirectly it correlates with negative ζ-potentials of the particles

Table 1 Basic characteristics of silver nanoparticle sols.

Sample preparation conditions		Mean size of nanoparticles according to DLS/nm	ζ-Potential/mV	Plasmon peak position according to UV-VIS spectroscopy/nm	pH of the solution
Solution volume of added silver oxide complex/ml	Reaction time/min				
0.1	20	23; 202	–35	412	8
0.5	20	2; 38; 409	–42	417	9
2.5	20	7; 92	–51	430	10
0.1	30	27; 158	–30	410	8
0.5	30	2; 40; 144	–42	425	9
2.5	30	11; 84	–49	443	10
0.1	60	26; 234	–41	412	7
0.5	60	40; 365	–44	427	7
2.5	60	87	–48	452	9

(Table 1) since NH_3 tends to absorb onto silver particle surfaces demanding a shell of hydroxyls around the nanoparticles. We believe that the presence of ammonia in the sols does not disturb at all in most of cases of practical applications of the sols since silver sols admixed to different buffer solutions prior, for example, SERS measurements of biological objects and this makes the toxicity of NH_3 negligible.

[†] In a typical PUSH preparation run, a 0.5 M aqueous sodium hydroxide solution was added dropwise to 20 ml of a freshly prepared 0.1 M aqueous silver nitrate solution until the complete precipitation of black-brown silver(I) oxide. Then, this as-prepared oxide was washed three times with deionized water (Milli-Q, Millipore) and dissolved in 5 ml of a 10% aqueous ammonia solution. The obtained transparent silver complex solution was filtered through Millex-LCR syringe driven filter units (Millipore, 0.45 μm pores). An aliquot portion of the resulting solution (0.1, 0.5 or 2.5 ml) was added to 50 ml of boiling deionized water, leading to decomposition of the silver complex: $4\,[Ag(NH_3)_2]OH = 4\,Ag + 8\,NH_3 + O_2 + 2\,H_2O$. After 20, 30 and 60 min of the decomposition reaction, the aliquots of silver nanoparticle sols were collected and immediately quenched down inside plastic Eppendorf tubes by cold water to store in a refrigerator at about 5 °C overnight. The overall concentration of silver in sols varied in the range of 0.2–5 mM.

The obtained silver nanoparticles were characterized by a transmission electron microscopy (TEM) and electron diffraction (ED) using a LEO912 AB OMEGA (Carl Zeiss) electron microscope. The UV-VIS absorption spectra were recorded using a Lambda 35 spectrophotometer (Perkin–Elmer). Zetasizer Nano ZS (Malvern Instruments) was used for dynamic light scattering (DLS) measurements of the particle size distribution and ζ-potentials. The pH of prepared solutions was estimated using a universal indicator paper.

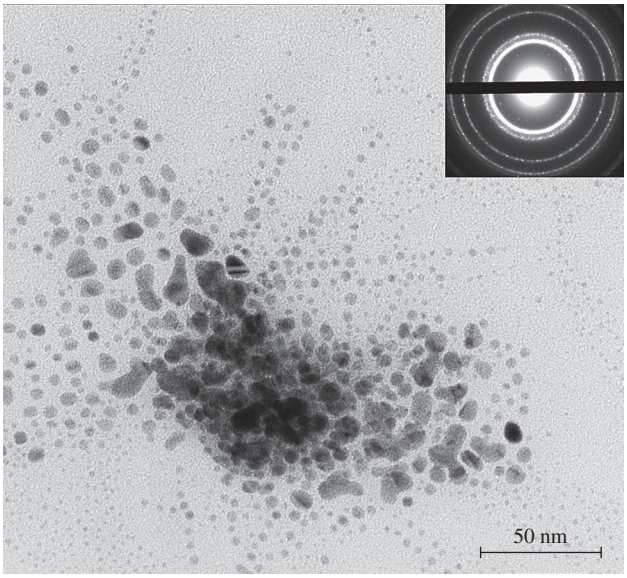

Figure 1 Typical TEM image and ED pattern (insert) of silver nanoparticles.

The special color of PUSH sols and their difference in reflection and transmission configurations originates from the presence of silver nanoparticle as clearly proved by TEM, ED, DLS and UV-VIS spectroscopy data (Figures 1–3, Table 1). Direct observations of silver precipitates by TEM at early stages of silver(I) oxide complex decomposition (Figure 1) show round-shaped nanoparticles with a bimodal size distribution. The major fraction possesses diameters within the range of 1–5 nm while a smaller amount of nanoparticles grows up to 20–30 nm and some of them have twin defects. The aggregation of nanoparticles is not observed.

A remarkable picture is given by DLS data. It is well-known that DLS results could overestimate the mean particle size of large objects compared to the real particle size distribution and also DLS often mimics broad distributions with a set of narrower DLS peaks. Nevertheless, Figure 2 shows that silver nanoparticles smaller than 10 nm can be found in as-prepared samples together with another, larger particle fraction; this is in a full agreement with TEM data (Figure 1). The observation is a reflection of expected nucleation-and-growth process features, probably, with an interference of diffusion rate limiting factors caused by the overlapping of diffusion fields around growth sites. Indeed, the first 10–15 min of colorless solution would correspond to the nucleation stage resulting in first embryocrystals of silver. Then, the growth process starts with the highest supersaturation and forces the first fraction of metallic silver to grow very quickly to the largest sizes thus diminishing local supersaturation. At the same time, the homogeneous nucleation of silver persists under the conditions of falling supersaturation and that permanently generates new growth sites composing the small particle fraction. Most probably, 100–200 nm particles grow much slower and become a final point of size evolution because of a smaller ratio of surface and volume for larger particles, while a supersaturation decrease in time prevents fast growth, as at the very beginning, making a 20–30 nm fraction dominant due to the evolution of the smallest particles. Actually, such bimodal particle distributions are not rare,[14] and they could be due to coupling between diffusion processes, including overlapping diffusion fields, and undercooling / supersaturation variation in time. It is known that this is caused, for example, by soft impingement, followed by a renewal of driving force for nucleation, with the subsequent soft impingement.[14] Under very high supersaturation, the particle size distribution becomes unimodal because supersaturation always outruns diffusion and the particle ensemble never reaches soft impingement.

These assumptions agree well with data shown in Figure 2. The smallest concentration of the silver(I) oxide complex (Figure 2, curves *1–3*) gives the smallest initial supersaturation; then, a smaller amount of 1–2 nm embryocrystals form a 20–30 nm fraction, which pumps silver into the final 200–300 nm fraction. The medium silver(I) oxide complex concentration keeps a permanently formed fraction of 1–2 nm nanoparticles since supersaturation is enough for that; then, a 20–30 nm fraction of silver nanoparticles remains together with the growing final 200–300 nm fraction. It is interesting but quite expected that the largest initial concentration of the decomposing complex generates the highest supersaturation, as compared to other samples. In turn, this gives the highest probability of the simultaneous formation of numerous nuclei and provides conditions for their simultaneous fast growth. It relaxes quickly entire supersaturation, quenches the formation of new embryocrystals; therefore, the whole silver nanoparticle ensemble jumps to the 100 nm size and stops to grow quickly since the particles have a more or less narrow size distribution function and there is no need for further quick evolution like in the previous cases. Similar results published elsewhere[15] except the application of hydrogen gas acting as a reducing agent. In our experiments no chemicals are used to reduce silver.

The finally collected ensembles of nanoparticles [Figure 3(*a*)] demonstrate different optical properties, all with clearly observed plasmonic peaks (PPs). The intensities of PPs increase with the reaction time and silver(I) oxide complex amount introduced in the reacting systems. This simply means that more silver scattering/absorption centers appeared in the sols. At the same time, the positions of PPs show a red shift coinciding with the change of particle sizes found in the sols by DLS (Figure 2, Table 1). The broad size distribution of silver nanoparticles leads to a highly asymmetrical UV-VIS absorption spectra with long tails towards larger wavelengths. The electrostatic stabilization of sols is provided by ζ-potentials of –35 to –50 mV found for the water-dispersed nanoparticles (Table 1). No sedimentation was observed at room temperature for at least two weeks in all of the cases. Moreover, freezing the colloid into ice, keeping it at –15 °C for

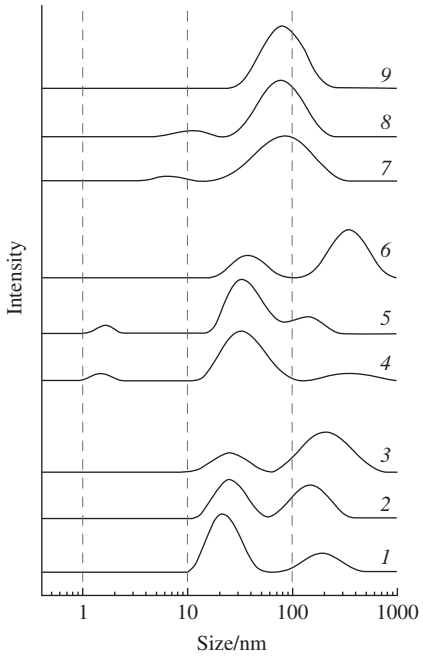

Figure 2 Evolution of particle sizes depending on reaction time and initial concentration of silver oxide complexes in the solution (DLS data). (*1*) 0.1 ml of added solution of silver oxide complex, 20 min of reaction time in boiling water, (*2*) 0.1 ml and 30 min, (*3*) 0.1 ml and 60 min, (*4*) 0.5 ml and 20 min, (*5*) 0.5 ml and 30 min, (*6*) 0.5 ml and 60 min, (*7*) 2.5 ml and 20 min, (*8*) 2.5 ml and 30 min and (*9*) 2.5 ml and 60 min.

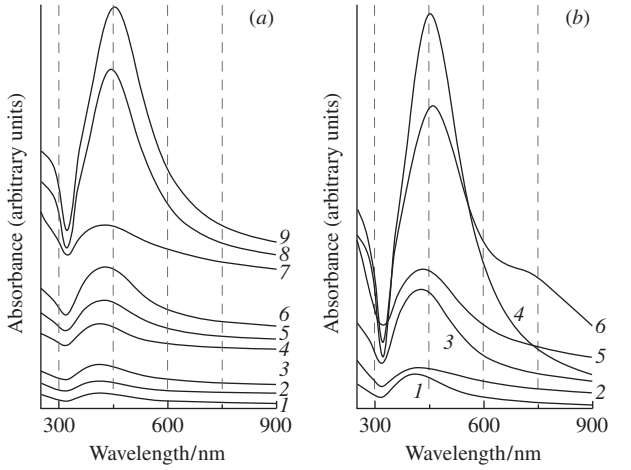

Figure 3 Evolution of plasmonic peak positions depending on reaction time and initial concentration of silver oxide complexes in the solution (UV-VIS spectroscopy data). (*a*) 0.1 ml of added solution of silver oxide complex after (*1*) 20, (*2*) 30 and (*3*) 60 min of reaction time in boiling water; 0.5 ml after (*4*) 20, (*5*) 30 and (*6*) 60 min; 2.5 ml after (*7*) 20, (*8*) 30 and (*9*) 60 min. (*b*) UV-VIS spectra of (*1*, *3*, *4*) as-prepared silver sols and (*2*, *5*, *6*) after 15 days of freezing the samples at –15 °C followed by iced sol melting and a short ultrasonic treatment. PUSH were prepared by addition of (*1*, *2*) 0.1, (*3*, *5*) 0.5, (*4*, *6*) 2.5 ml of the silver oxide complex into hot water (60 min of reaction time series).

15 days and melting the iced sols followed by their ultrasonic treatment for 10 min resulted in the almost complete restoration of sol colors and their absorption spectra, as shown in Figure 3(*b*).

Thus, a new simple user-friendly method of pure silver hydrosol preparation is suggested. Such PUSH samples are very attractive in the field of SERS measurements of biological objects[16] since the method is highly reproducible, gives no by-products and produces stable sols of almost naked silver nanoparticles with effective absorption and asymmetric PP spectra. Pure silver hydrosols are suitable for practical biomedical applications since they can be stored for a long time in a frozen state with the complete restoration of their properties afterward, and they do not change the natural environment of biological objects due to the absence of toxic stabilizing agents or impurities.

This work was supported by the Russian Foundation for Basic Research (grant nos. 10-03-00976-a and 11-03-00761-a). We are grateful to V. K. Ivanov (N. S. Kurnakov Institute of General and Inorganic Chemistry, Russian Academy of Sciences) for fruitful discussions.

References

1 T. Huang and X.-H. N. Xu, *J. Mater. Chem.*, 2010, **20**, 9867.
2 A. Pyatenko, M. Yamaguchi and M. Suzuki, *J. Phys. Chem. C*, 2007, **111**, 7910.
3 X. K. Meng, S. C. Tang and S. Vongehr, *J. Mater. Sci. Technol.*, 2010, **26**, 487.
4 B. Wiley, Y. Sun, B. Mayers and Y. Xia, *Chem. Eur. J.*, 2005, **11**, 454.
5 S. Peng and Y. Sun, *Chem. Mater.*, 2010, **22**, 6272.
6 B. Pietrobon and V. Kitaev, *Chem. Mater.*, 2008, **20**, 5186.
7 V. K. Sharma, R. A. Yngard and Y. Lin, *Adv. Colloid Interface Sci.*, 2009, **145**, 83.
8 M. Ahamed, M. S. AlSalhi and M. K. J. Siddiqui, *Clin. Chim. Acta*, 2010, **411**, 1841.
9 K. Chaloupka, Y. Malam and A. M. Seifalian, *Trends Biotechnol.*, 2010, **28**, 580.
10 S. Feng, R. Chen, J. Lin, J. Pan, G. Chen, Y. Li, M. Cheng, Z. Huang, J. Chen and H. Zeng, *Biosens. Bioelectron.*, 2010, **25**, 2414.
11 N. A. Brazhe, S. Abdali, A. R. Brazhe, O. G. Luneva, N. Y. Bryzgalova, E. Y. Parshina, O. V. Sosnovtseva and G. V. Maksimov, *Biophys. J.*, 2009, **97**, 3206.
12 J. Fang, S. Liu and Z. Li, *Biomaterials*, 2011, **32**, 4877.
13 G. Brauer, *Handbuch der Präparativen Anorganischen Chemie*, Ferdinand Enke Verlag, Stuttgart, 1975, p. 998 (in German).
14 Y. H. Wen, J. P. Simmons, C. Shen, C. Woodward and Y. Wang, *Acta Mater.*, 2003, **51**, 1123.
15 D. D. Jr. Evanoff and G. Chumanov, *J. Phys. Chem.*, 2004, **108**, 13948.
16 X. Guangnian, Q. Xueliang, Q. Xiaolin and C. Jianguo, *Rare Met. Mater. Eng.*, 2010, **39**, 1532.

Received: 11th July 2011; Com. 11/3760